J. Plasma Fusion Res. SERIES, Vol. 4 (2001) 239–242

Pedestal Structure and Thermal Energy Confinement of ELMy H-mode in JT-60U

URANO Hajime*, KAMADA Yutaka[1], KUBO Hirotaka[1], SAKURAI Shinji[1], SHIRAI Hiroshi[1], TAKIZUKA Tomonori[1], HATAE Takaki[1], IDE Shunsuke[1], FUJITA Takaaki[1] and FUKUDA Takeshi[1]

Graduate School of Engineering, Hokkaido University, Sapporo 060-8628, Japan

[1] Naka Fusion Research Establishment, Japan Atomic Energy Research Institute, Ibaraki 311-0193, Japan

(Received: 5 December 2000 / Accepted: 17 August 2001)

Abstract

A role of the pedestal temperature as a boundary condition in determining the energy confinement of the plasma core was analyzed by comparing between D_2 and D_2 + Ar gas puffed ELMy H-mode discharges in JT-60U. As the density is raised during ELMy H-mode, the pedestal temperature drops so that the pedestal pressure remains constant. Externally puffed seed impurity leads to the center-peaked density profiles as well as a slight reduction in the thermal ion density, and the reduction in the pedestal temperature weakened at a high density. Since the temperature profiles were approximately self-similar, the thermal conductivity was reduced consistently with the temperature at the plasma boundary even with and without Ar injection.

Keywords:

ELMy H-mode, profile similarity, pedestal temperature, Ar injection and JT-60U

1. Introduction

While it has been proved possible in present day experiments to demonstrate high density operation modes that lower the peak heat flux onto the divertor plates sufficiently for a tokamak reactor [1], it has generally been seen that such regimes also have diminished core plasma confinement quality [2-4]. Much attention therefore has focused on the clarification of the dominant causes of this confinement degradation in ELMy H-mode plasmas. A role of the pedestal structure determined by the ELM activities is seen to be significant for the thermal transport of the plasma core [3,5-8]. However, numerous edge pedestal quantities, such as the density and temperature, which tend to vary monotonically together, prevent us from revealing the decisive factor of the boundary condition. In this paper, focusing on externally Ar gas puffed discharges that are seen to be of great use to the energy confinement improvement with high radiation loss power in a high density regime [9-12], the boundary condition for core confinement is analyzed in ELMy H-mode plasmas on JT-60U.

2. Density Dependence of Thermal Energy Confinement

ELMy H-mode experiments were performed with and without Ar gas injection in JT-60U at I_p = 1.2 MA, where the Greenwald density limit, n^{GW}, corresponds to (5.4–5.8) × 10^{19} m^{-3} [10]. The toroidal magnetic field, B_t = 2.5–2.6 T and the safety factor at the 95 % of flux surface, q_{95} = 3.3–3.6. Neutral beam (NB) of deuterium was injected into deuterium plasma at P_{NBI} of 16–18 MW. In a series of experiments without Ar gas injection, the line-averaged electron density measured with FIR interferometer, $\bar{n}_e$, was varied from 2.5 × 10^{19}

Corresponding author's e-mail: urano@fusion.qe.eng.hokudai.ac.jp

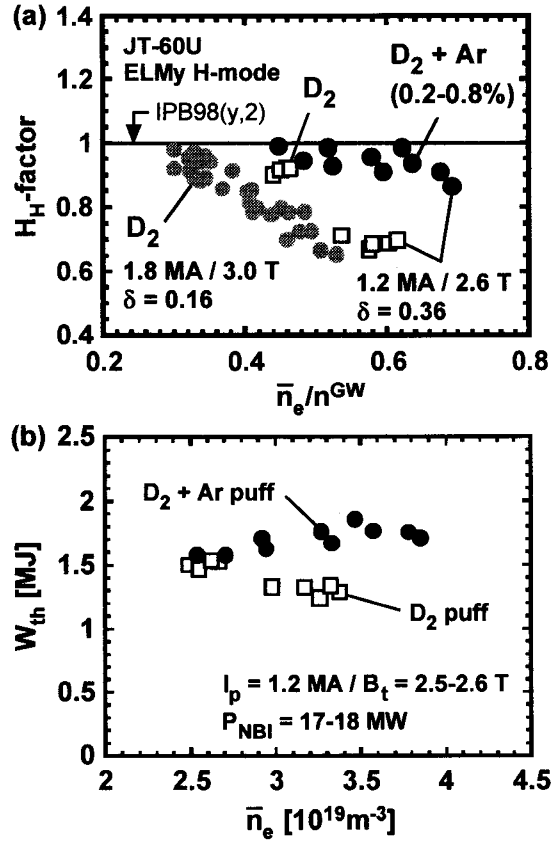

Fig. 1 (a) H_H-factors for ELMy H-mode discharges in JT-60U as a function of n_e/n^{GW}. Open squares and closed circles indicate the H-factors in the discharges at I_p = 1.2 MA and B_t = 2.5–2.6 T with and without Ar injection, respectively. Shaded circles indicate the discharges at I_p = 1.8 MA and B_t = 3.0 T only with deuterium gas puffing. (b) Density dependence of W_{th}.

to 3.4 × 10^{19} m^{-3}. In Ar gas injected discharges, $\bar{n}_e$ increased to 3.9 × 10^{19} m^{-3}. The maximum $\bar{n}_e$ reached was 0.69 × n^{GW}. As the density is raised with Ar gas puffing, the effective charge number, Z_{eff}, increased from 2.5 to 4.9, while it ranged with a scatter between 2.1 and 2.5 without Ar injection. Elongation, κ, of 1.4 and triangularity, δ, of 0.35–0.36 were fixed. The plasma volume, V_p, was in the range of 57–58 m^3. The plasma major radius, R_p, and the minor radius, a_p, were in the ranges of 3.35–3.38 m and of 0.82–0.83 m, respectively.

Figure 1(a) shows that the H_H-factor, defined as thermal energy confinement time, τ_{th}, normalized to the IPB98(y,2) scaling [13], as a function of $\bar{n}_e/n^{GW}$. In D_2 gas puffed plasmas at I_p of 1.2 MA (open squares), the H_H-factor decreases continuously from 0.9 to 0.7 with

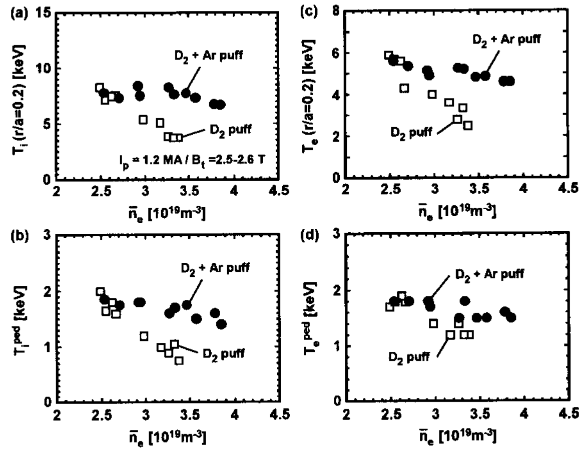

Fig. 2 Density dependence of (a) T_i (r/a = 0.2), (b) T_i^{ped}, (c) T_e (r/a = 0.2) and (d) T_e^{ped} in ELMy H-mode discharges with and without Ar injection.

increasing $\bar{n}_e/n^{GW}$ from 0.44 to 0.61. On the other hand, in Ar injected discharges (closed circles), the H_H-factor remains in the range of 0.9–1.0 until $\bar{n}_e/n^{GW}$ reaches 0.64, and then the H_H-factor declines gradually with a further increase in density. Figure 1(b) indicates the density dependence of thermal stored energy, W_{th}. As $\bar{n}_e$ is increased, W_{th} decreases gradually to 1.2 MJ in D_2 gas puffed discharges, while it increases to 1.9 MJ in Ar injected plasmas.

Figure 2(a) and (b) plot the ion temperatures at the shoulder of the H-mode pedestal, T_i^{ped}, and near the center, $T_i(r/a = 0.2)$, as a function of $\bar{n}_e$, respectively. It is observed in D_2 gas puffed plasmas that both T_i^{ped} and $T_i(r/a = 0.2)$ decrease continuously with increasing $\bar{n}_e$. However, it can be seen in Ar seeded case that the reduction in T_i^{ped} due to an increase in density weakens in comparison with the case without Ar injection. The core temperature, $T_i(r/a = 0.2)$, also tends to decrease slowly with an increase in density. The similar behavior is also seen in the electron temperatures as shown in figure 2(c) and (d). Besides, it may be worth pointing out, in passing, that the electron density profiles with Ar injection tend to be peaked at the center. In the plasma with Ar injection, while the radiative loss power is predominantly enhanced in the edge region, the power radiated from the region of r/a < 0.6, which is several times larger than that without Ar injection, is ~10 % of the heating power injected into the region.

As $\bar{n}_e$ is raised with increasing the Ar concentration, f_{Ar}, from 0.2 to 0.8 %, the dilution of thermal deuterium ions is enhanced gradually by 10 %, i.e., the fraction of thermal deuterium, f_D^{th}, decreases from 60 to

50 %. The fraction of carbon density, f_C, remains constant in the range of 4–6 %. On the other hand, f_D^{th} and f_C are in the ranges of 70–79 % and 4–5 % in the discharges without Ar gas injection, respectively. The energy confinement due to Ar gas injection is improved more than the compensation for the dilution of deuterium because H_H-factor is higher than the discharges without Ar injection by ~ 30 % at $\bar{n}_e/n^{GW}$ of 0.6 as shown in figure 1(a).

3. Pedestal Structure during ELMy H-mode

As $\bar{n}_e$ is increased without impurity gas injection, the temperature at the pedestal shoulder drops as shown in figure 2(b) and (d). This reduction in the temperature seems to be determined as a pedestal structure by the ELM activities. In figure 3, the pedestal pressures, p_{ped}, are plotted in ELMy H-mode plasmas with and without Ar injection as a function of $\bar{n}_e$. The pedestal pressure, p_{ped}, is evaluated as:

$$p_{ped} = n_e^{ped} k_B \left(T_e^{ped} + \sum_j f_j T_j^{ped} \right) \qquad (1)$$

where f_j denotes the fraction of density for each thermal ion species. It is observed in Ar injected plasmas that p_{ped} is kept constant in the range of 6.5–8.0 × 10^3 Pa over a wide range of density. Compared with D_2 gas puffed discharges, higher p_{ped} (~ 8 %) is obtained in Ar injected plasmas. As the density is increased with Ar injection, the thermal ion density decreases slightly and the peaked density profiles are sustained, and thus the reduction in the pedestal temperature weakens so that p_{ped} remains constant.

4. Boundary Condition for Core Confinement

It has been observed that the pedestal structure determined by the destabilization of ELMs has a large influence on thermal energy confinement of the plasma core. In particular, since the pedestal density and temperature vary inversely in the ELMy phase without impurity gas injection, the confinement degradation at a high density can be linked to the relatively low pedestal temperatures.

The effective thermal conductivity of the plasma core, χ_{eff}^{core}, evaluated as:

$$\chi_{eff}^{core} = \frac{\int_0^{r_{ped}} \chi_{eff}(r) \cdot 2\pi r dr}{\int_0^{r_{ped}} 2\pi r dr} \qquad (2)$$

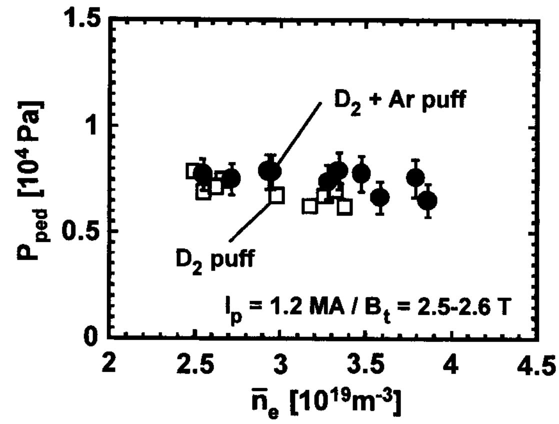

Fig. 3 Dependence of the edge pedestal pressure upon density.

is plotted as a function of T_i^{ped} in figure 4(a). In Eq. (2), $\chi_{eff}(r)$ is calculated by the transport analysis code for thermal plasmas (TOPICS) [14]. It can be seen that χ_{eff}^{core} tends to be reduced gradually with increasing T_i^{ped}. It is the most significant feature in figure 4(a) that the trend of χ_{eff}^{core} on T_i^{ped} is conformed consistently to the Ar gas injected plasmas. This finding might be indicative of a profile similarity of the temperatures, which suggests the existence of a relationship between edge profiles and core confinement. In this series of discharges, the core temperatures are seen to increase approximately proportional to the pedestal temperatures as shown in figure 4(b). The pedestal temperature might play a role as a boundary condition for core confinement because the temperature profiles are approximately self-similar and differ only by a constant factor. If the achievable pedestal pressure is limited by the ELM activities, the pedestal temperature can also be determined by the pedestal density for each species. Externally Ar gas puffed plasmas lead to a slight reduction in the thermal ion density and the center-peaked density profiles, in which the pedestal density becomes lower than that of plasmas without Ar injection at fixed $\bar{n}_e$. Therefore, the reduction in the pedestal temperature weakens at a high density so that p_{ped} remains constant. Figure 4(c) shows that the temperature profiles of high density Ar gas injected plasma ($\bar{n}_e/n^{GW}$ ~ 0.60) are similar to those of low density plasma without Ar gas ($\bar{n}_e/n^{GW}$ ~ 0.45). The highly achieved pedestal temperature due to Ar gas injection can produce high core temperature leading to the improvement of the energy confinement.

5. Conclusions

The dominant factor at the plasma boundary for the

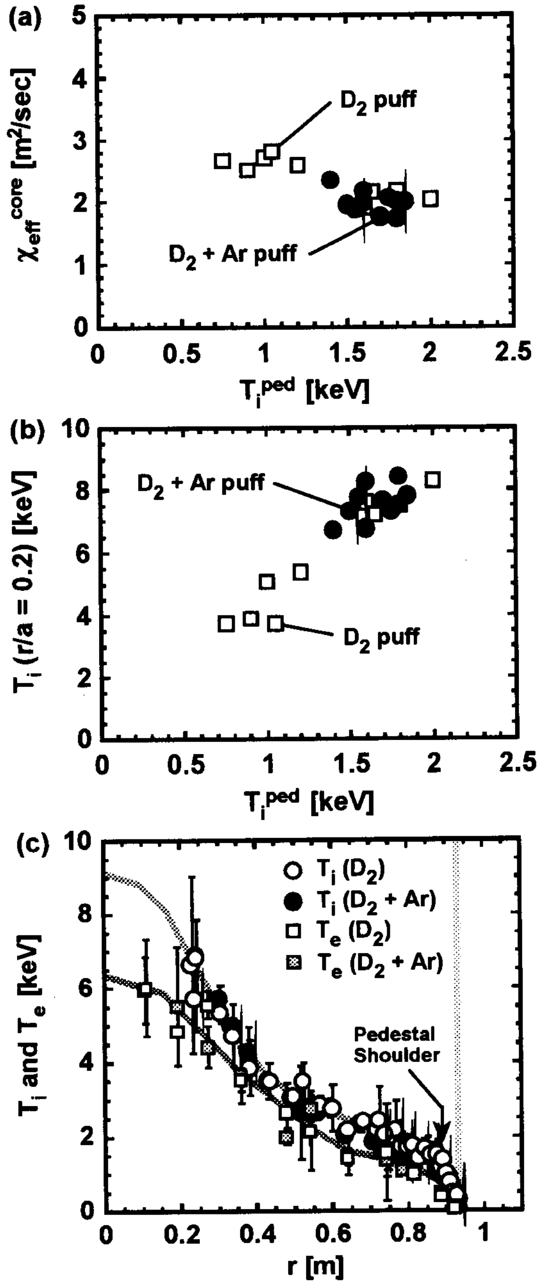

Fig. 4 (a) Dependence of χ_{eff}^{core} on T_i^{ped} in ELMy H-mode plasmas. (b) Relationship between the core and pedestal temperatures. (c) Profile similarity between a high density Ar gas injected plasma ($n_e/n^{GW} \sim 0.60$) and a low density plasma without Ar gas ($n_e/n^{GW} \sim 0.45$).

thermal energy confinement of the plasma core was analyzed in the ELMy H-mode plasmas on JT-60U. The core temperatures were observed to increase in proportion to the pedestal temperatures. Externally puffed seed impurity leads to the center-peaked density profiles as well as a slight reduction in the thermal ion density. Thus, the reduction in the pedestal temperature in Ar gas puffed plasmas weakened so that the pedestal pressure was kept almost constant over a wide range of density. The dependence of the thermal conductivity of the plasma core on the pedestal temperature was conformed consistently to the Ar gas puffed plasmas.

Acknowledgements

The authors are grateful to Drs. H. Ninomiya, K. Ushigusa and Y. Miura of Japan Atomic Energy Research Institute for many fruitful discussions on the subject. One of the authors (H. Urano) would like to express his gratitude to Professor M. Itagaki of Hokkaido University, whose encouragement and advice were invaluable.

References

[1] G. Janeschitz *et al.*, in Fusion Energy 1996 (*Proc. 16th Int. Conf.* Montreal, 1996), Vol. 2, IAEA, Vienna, 755 (1997).

[2] JET Team, Nucl. Fusion **39**, 1687 (1999).

[3] W. Suttrop, F. Ryter and V. Mertens *et al.*, in Fusion Energy 1998 (*Proc. 17th Int. Conf.* Yokohama, 1998), Vol. 2, IAEA, Vienna, 777 (1999).

[4] N. Asakura *et al.*, Plasma Phys. Control. Fusion **39**, 1295 (1997).

[5] M. Greenwald *et al.*, Nucl. Fusion **37**, 793 (1997).

[6] W. Suttrop *et al.*, Plasma Phys. Control. Fusion **39**, 2051 (1997).

[7] G. Janeschitz *et al.*, in Control. Fusion and Plasma Physics (*Proc. 26th Eur. Conf.* Maastricht, 1999), Vol. 23J, European Physical Society, Geneva (1999) 1445.

[8] H. Urano *et al.*, Nucl. Fusion **42**, (2002) (in press).

[9] H. Kubo *et al.*, *Proc. 18th Int. Conf. on Fusion Energy*, Sorrento, IAEA-CN-77/EX5/3 (2000).

[10] S. Sakurai *et al.*, J. Nucl. Mater. **290-293**, 1002 (2001).

[11] R.R. Weynants, Nucl. Fusion **39**, 1637 (1999).

[12] G.L. Jackson *et al.*, J. Nucl. Mater. **266-269**, 380 (1999).

[13] ITER Physics Expert Groups on Confinement and Transport and Confinement Modelling and Database, ITER Physics Basis Editors, Nucl. Fusion **39**, 2175 (1999).

[14] H. Shirai *et al.*, Plasma Phys. Control. Fusion **42**, 1193 (2000).